

Social Housing: Critical Evaluation of Prestress Losses in Precast Slabs

Bolívar Hernán Maza¹, Daniela Stefanía Maza Vivanco², Dolores Maza Vivanco³

¹Universidad Técnica Particular de Loja
San Cayetano Alto, Loja, Ecuador
bhmaza@utpl.edu.ec

²Universidad Técnica Particular de Loja
San Cayetano Alto, Loja, Ecuador
dsmaza@utpl.edu.ec

³Escuela Superior Politécnica Agropecuaria de Manabí
Calceta, Manabí, Ecuador
dvmaza@espam.edu.ec

Abstract - Prestressed concrete involves artificially inducing controlled stresses by means of high-tensile steel cables in the opposite direction to the stresses caused by applied loads. These compressions, superimposed on the tensile stresses induced by applied loads, create a total stress state within limits that concrete can withstand indefinitely. Prestressing does have drawbacks, such as stress losses, which are strategically managed. Delayed losses due to concrete creep are evaluated using the formula: $\Delta f_{CR} = \frac{2E_p}{E_c} (f_{cir} - \frac{M_{ds}}{I_{pl}} e_o)$

Stress losses due to steel relaxation are evaluated using the expression: $\Delta f_{RE} = C[K_{re} - J(\Delta f_{ES} + \Delta f_{CR} + \Delta f_{SH})]$

The objective is to assess the stress losses in both steel and concrete to ensure the structural operational life. It was found that the losses due to concrete shrinkage and steel relaxation are small, particularly when they are deferred. There is a need to distinguish between transfer sections and critical sections, tentatively located at a distance of 1/4 from the support. In the case of the PPCC:6/60:30 type precast slab, the only one where, due to wire eccentricity, a convex deflection may occur upon the transfer of prestressing. It is reported that the result is valid for the industrialisation of the PPCC model.

Keywords: Steel relaxation; Concrete plastic Flow; Prestress losses; Precast slabs.

1. Introduction

The stretching of the High Tensile Strength Cable (HTSC) causes friction with the duct in areas where the cable changes direction, which induces significant tension losses [1]; [2]. During the transfer of energy from the HTSC to the concrete, the concrete compresses or shortens, and as a result, the tension in the cable is evidently reduced. The concrete compresses, leading to a reduction in cable tension due to the shortening of the concrete element [3]; [4]. The anchoring elements (cones, wedges, etc.) shift after tensioning, causing tension drops in the cable [2]. Deferred tension losses in the HTSC are related to the properties of the steel and concrete. The steel may undergo creep and relaxation, similarly to the concrete. Prestressed steel, acting as active reinforcement over time, relaxes and loses tension [5]. Concrete, under constant service loads over time, induces tension losses in the cables [1].

In this context, significant tension losses in HTSC can lead to a reduction in the load-bearing capacity of the prestressed element, potentially resulting in the premature loss of the operational lifespan of the prestressed structure. Tension losses in the HTSC can trigger a significant reduction in the load-bearing capacity of prestressed concrete beams or result in inadequate structural performance under service loads [6]. The reduction in tension in the HTSC decreases the durability of the prestressed structure in the medium and long term, potentially leading to cracking and, consequently, the depassivation of the steel [3]; [6]. The relaxation of the steel and the loss of tension increase deformations in the prestressed beams; in this case, the structure will reduce its serviceability and may operate under high risk of total collapse [7]; [8]. In this sense, the context provides sufficient reason to investigate and offer a summary of all (initial and deferred) losses assessed in the extreme section of the transition zone, as well as those occurring in the central region of the element, for the 48 precast slabs

that form the database of this research. The user can conceive of any other deferred typology. The fundamental objective of this research is to assess the initial losses ($\Delta f_{initial}$) and deferred losses ($\Delta f_{deferred}$) in high tensile strength cables embedded in the concrete as active reinforcement. The identification of the factors involved in both initial and deferred losses fundamentally depends on the type of prestressing being analysed (pre-tensioning or post-tensioning), and its assessment is fraught with uncertainties due to the number of variables involved, namely: the equipment used to perform the tensioning, the effectiveness of the anchoring system used to hold the initial tension applied to the steel, the type of steel being stretched and especially its degree of relaxation, as well as time-dependent and deferred phenomena such as concrete shrinkage and creep over which the prestressing is transferred, etc.

2. Materials

It is possible to estimate loss values that can be reasonably accurate based on considerations of the initial stress level ($f_{pi} \geq 0.70f_{pu}$) the type of steel used (stress-relieved or low-relaxation; whether it is wire, tendon, or bar), the exposure conditions of the element, especially the ambient humidity surrounding the piece during its service life, the technique employed (pre-tensioning, post-tensioning with or without bonding), etc. Undoubtedly, this estimation greatly depends on the experience of the person conducting it; however, codes and technical documents related to the subject offer more or less accurate analytical models that help improve the effectiveness of such an estimation. For the type of element under analysis, there is no precedent to establish an accurate estimator to quantify the tension losses that occur, which justifies the extensive study.

In this work, the prestressed structural element under analysis is a floor and roof slab used as a horizontal structural solution for Social Housing (VIS). In the precast slab, the steel is stretched and anchored before the concrete is poured (pre-tensioning); consequently, initial losses due to friction do not occur ($\Delta f_{FR} = 0$)^①, nor do losses due to wedge seating, penetration, or slip during transfer ($\Delta f_{PA} = 0$)^②. However, when the cables are cut, there is an immediate elastic shortening of the concrete, causing the initial loss known as elastic shortening ($\Delta f_{ES} \neq 0$)^③.

Meanwhile, the deferred losses are fundamentally due to the relaxation of the steel ($\Delta f_{RE} \neq 0$)^④, depending on its relaxation grade, as well as the shrinkage ($\Delta f_{SH} \neq 0$)^⑤ and creep ($\Delta f_{CR} \neq 0$)^⑥ of the concrete. Therefore, in the case of the precast slab, the following tension losses need to be quantified:

$$\Delta f_{initial} = \overset{0}{\Delta f_{FR}} + \overset{0}{\Delta f_{PA}} + \Delta f_{ES} = \Delta f_{ES} \quad (1)$$

The subscripts used to identify each of the losses that will be evaluated are defined as follows:

- ES: Elastic Shortening (acortamiento elástico)
- CR: Creep (concrete creep; "arrastre" or creep of the concrete)
- SH: Shrinkage (shrinkage of the concrete; "encogimiento", shrinkage, or contraction of the concrete)
- RE: Relaxation (steel relaxation; relajación del acero)

If f_{pj} denotes the initial tension to which the steel is stretched (corresponding to the force P_j), when the initial losses associated with the tensioning, anchoring, and transfer process occur, this tension drops to the value f_{pi} (associated with the force P_i), until it finally stabilises at an effective tension value f_{pe} (corresponding to the force P_e) as the deferred losses, which are time-dependent, take place. The following diagram illustrates this concept:

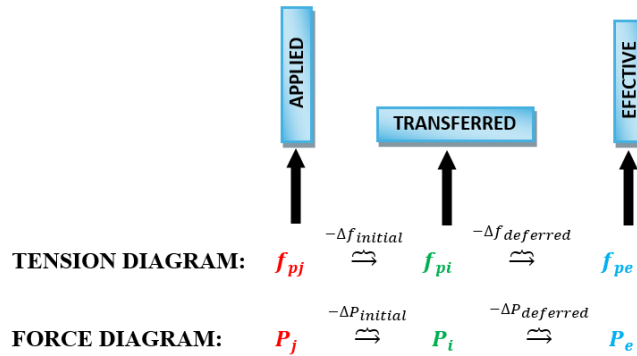


Fig. 1: Diagram Tension and Force

3. Methodology

To evaluate the tension losses in the steel, this work will adopt the analytical model suggested by the PCI in the Second Edition of the Manual for the Design of Hollow Core Slabs. The evaluation requires the definition of the following elements:

- Geometric characteristics of the cross-section where the prestressing is transferred (based on its dimensions).
- Sections where the compliance with tension requirements must be verified.
- Analytical expressions to quantify each loss.

Table 1: summarises the geometric characteristics of the Prestressed Precast Slab with Composite Topping (PPCC) model.

GEOMETRIC CHARACTERISTICS OF PPCC: ($b = 495\text{mm}$) y ($r_c = h_2 = 30\text{mm}$)									
h_1 (mm)	h_{pl} (mm)	A_{pl} (mm^2)	\bar{h}_{pl} (mm)	v_{pl} (mm)	v'_{pl} (mm)	I_{pl} (mm^4)	W_{pl} (mm^3)	W'_{pl} (mm^3)	q_{pl} (kg/m)
30	60	21 218	42.9	37.0	23.0	4 333 521	117 261	-188 055	50.9
35	65	23 693	47.9	39.6	25.4	5 784 897	145 993	-227 971	56.9
40	70	26 168	52.9	42.3	27.7	7 531 343	178 210	-271 507	62.8

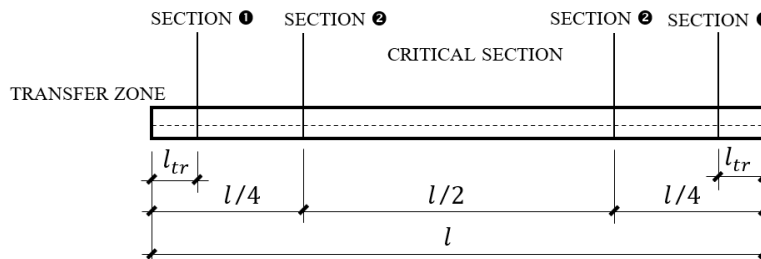


Fig. 1: Detensioning Sections.

Several authors are using the Model Code CEB-FIP method to evaluate the transfer length of energy in prestressed elements due to its accuracy in results [9]; [10]. The Model Code CEB-FIP model for evaluating transfer length has proven to deliver precise and relevant results, experimentally verified [11]. The transfer zone corresponds to the length (l_{tr}), defined as the minimum length required by a bonded tendon to transmit the prestressing force to the concrete section. Beyond this length, the prestressing force along the tendon can be considered constant for any time t at which it is evaluated, up to the transfer zone at the opposite end of the tendon, where the phenomenon occurs in the reverse direction.

Different models are known for evaluating the transfer length l_{tr} . This work adopts the method suggested by the MODEL CODE CEB-FIP, which defines it as follows:

$$l_{tr} = \alpha_1 \alpha_2 \alpha_3 \frac{f_{pj}}{f_{pu}} (l_{pd}) \quad (2)$$

Where:

- $\alpha_1: \left(\begin{array}{l} \mathbf{1.0} \text{ For slow transfer} \\ \mathbf{1.25} \text{ For sudden transfer, cutting of reinforcement} \end{array} \right)$
- $\alpha_2: \left(\begin{array}{l} \mathbf{1.0} \text{ For calculation under shear stress} \\ \mathbf{0.5} \text{ For calculation of transverse reinforcement in the anchorage zone} \end{array} \right)$
- $\alpha_3: \left(\begin{array}{l} \mathbf{0.7} \text{ For wires} \\ \mathbf{0.5} \text{ For strands} \end{array} \right)$
- $f_{pj} = \lambda_t f_{pu}$

$$\lambda_t: \left\{ \begin{array}{l} \mathbf{0.80} \text{ For low – relaxation wires with } \xi = \mathbf{0.90} \\ \mathbf{0.80} \text{ For stress – relieved wires with } \xi = \mathbf{0.85} \\ \mathbf{0.75} \text{ For formed bars with } \xi = \mathbf{0.80} \end{array} \right.$$

$$\xi = f_{py} / f_{pu} \text{ }^1 \quad (3)$$

Since wires are used in the reinforcement of the precast slab, and assuming that the steel has $\xi=0.85$ (one of the most common in the market), a value of $\lambda_t = 0.80$ will be adopted

$$l_{pd} = \frac{a_p}{p} \left(\frac{1.5}{\eta_1 \eta_2} \right) \frac{f_{py}}{f'_{cj}} \quad (4)$$

l_{pd} : Basic anchorage length of the wire

a_p : Area of the largest diameter wire used in the same precast slab

p : Bonded perimeter of the largest diameter wire used in the same precast slab

$$\eta_1: \left(\begin{array}{l} \mathbf{1.4} \text{ For wires} \\ \mathbf{1.2} \text{ For strands} \end{array} \right)$$

¹ It is common for this value to be specified by the manufacturer that produces the steel.

$$\eta_2: \begin{pmatrix} 1.0 \text{ For wires located less than 250 mm from the bottom of the piece, or more} \\ \text{than 300 mm below the top surface of concreting} \\ \text{For all other positions} \\ 0.7 \text{ For all other positions} \end{pmatrix}$$

3.1. Solution Determination of the transfer length for the precast slab

Concrete:

- Characteristic strength at 28 days $f'_c = 25 \text{ MPa}$
- Detensioning three days after pouring the concrete: $j = 3$

Steel:

- Ultimate strength: $f_{pu} = 1770 \text{ MPa}$
- Diameter: 3 mm
- $\xi = f_{py}/f_{pu} = 0.85 \Rightarrow \lambda_t = 0.80$

Solution

Set the values of the coefficients involved in the model:

- $\alpha_1 = 1.25$ (Sudden transfer of prestressing due to the type of cutting used)
- $\alpha_2 = 1.00$ (No transverse reinforcement will be used in the precast slab)
- $\alpha_3 = 0.70$ (This refers to wires and not strands)
- $n_1 = 1.4$ (This refers to wires and not strands)
- $n_2 = 1.00$ (The total thickness of the precast slab, for any of the typologies defined, is so thin that in all cases the steel is located at a distance much less than 25 cm from the bottom of the slab)

1) Definition of Steel Stress at the Time of Transfer (f_{pj})

For wire with $\xi = 0.85$ it is given by:

$$f_{pj} = \lambda_t f_{pu} = 0.80 f_{pu} = (0.80)(1770 \text{ MPa}) = 1416 \text{ MPa}$$

2) Definition of the Basic Anchorage Length for the Wire (l_{pd})

The concrete strength at the time of release, f'_{cj} is given by:²

$$f_{py} = \xi \cdot f_{pu} = 0.85(1770 \text{ MPa}) = 1504 \text{ MPa}$$

² For a relative humidity of $HR \geq 90\%$ and a temperature of $T \approx 20^\circ \text{C}$, the coefficient $\beta_{(j)}$ is given by:

$$\therefore l_{pd} = \frac{7.07mm^2}{18.8mm} \left[\frac{1.5}{(1.4)(1.0)} \right] \frac{1504MPa}{15MPa} = 40mm$$

3) Definition of Transfer Length (l_{tr})

$$l_{tr} = (1.25)(1.0)(0.70) \frac{1416MPa}{1770MPa} (40mm) = 28mm$$

This means that, in the case considered, at approximately 3 cm from both ends of the precast slab, the prestressing force can be considered constant. If this same procedure is applied to the remaining reinforcement typologies that have already been defined (diameter and steel strength), the results shown in Table 2 are obtained for the two types of HTSC.

Tabl 2. Results of l_{tr}

f_{pu} MPa	$d_b máx.$ mm	l_{tr} mm
1 770	3	28
	5	47
1860	3	30
	5	50

Table 3. Values for the characterization of the PPCC models.

PPCC					A_{pl} (mm ²)	I_{pl} (mm ⁴)	p_{pl} (mm)
	$d_b(max)$ (mm)	a_p (mm ²)	p (mm)	e_o (mm)			
$f_{pu} = 1770MPa$							
6/60:30:T-3 ³ /1770	3	7.07	18.80	-2	21 218	4 333 521	1 255
6/60:30:T-5 ³ /1770	5	19.64	31.42				
6/60:30:T-3 ⁵ /1770	3	7.07	18.80				
6/60:30:T-5 ⁵ /1770	5	19.64	31.42				
6/60:30:T-3 ² :5 ¹ /1770	5	19.64	31.42				
6/60:30:T-3 ¹ :5 ² /1770	5	19.64	31.42	0	23 693	5 784 897	1 265
6/60:30:T-3 ³ :5 ² /1770	5	19.64	31.42				
6/60:30:T-3 ² :5 ³ /1770	5	19.64	31.42				
6/60:35:T-3 ³ /1770	3	7.07	18.80				
6/60:35:T-5 ³ /1770	5	19.64	31.42				
6/60:35:T-3 ⁵ /1770	3	7.07	18.80	0	23 693	5 784 897	1 265
6/60:35:T-5 ⁵ /1770	5	19.64	31.42				
6/60:35:T-3 ² :5 ¹ /1770	5	19.64	31.42				
6/60:35:T-3 ¹ :5 ² /1770	5	19.64	31.42				
6/60:35:T-3 ³ :5 ² /1770	5	19.64	31.42				
6/60:35:T-3 ² :5 ³ /1770	5	19.64	31.42				

6/60:40:T-3 ³ /1770	3	7.07	18.80	0	26 168	7 531 343	1 275
6/60:40:T-5 ³ /1770	5	19.64	31.42				
6/60:40:T-3 ⁵ /1770	3	7.07	18.80				
6/60:40:T-5 ⁵ /1770	5	19.64	31.42				
6/60:40:T-3 ² :5 ¹ /1770	5	19.64	31.42				
6/60:40:T-3 ¹ :5 ² /1770	5	19.64	31.42				
6/60:40:T-3 ³ :5 ² /1770	5	19.64	31.42				
6/60:40:T-3 ² :5 ³ /1770	5	19.64	31.42				
$f_{pu} = 1\ 860\text{MPa}$							
6/60:30:T-3 ³ /1860	3	7.07	18.80	-2	21 218	4 333 521	1 255
6/60:30:T-5 ³ /1860	5	19.64	31.42				
6/60:30:T-3 ⁵ /1860	3	7.07	18.80				
6/60:30:T-5 ⁵ /1860	5	19.64	31.42				
6/60:30:T-3 ² :5 ¹ /1860	5	19.64	31.42				
6/60:30:T-3 ¹ :5 ² /1860	5	19.64	31.42				
6/60:30:T-3 ³ :5 ² /1860	5	19.64	31.42				
6/60:30:T-3 ² :5 ³ /1860	5	19.64	31.42				
6/60:35:T-3 ³ /1860	3	7.07	18.80	0	23 693	5 784 897	1 265
6/60:35:T-5 ³ /1860	5	19.64	31.42				
6/60:35:T-3 ⁵ /1860	3	7.07	18.80				
6/60:35:T-5 ⁵ /1860	5	19.64	31.42				
6/60:35:T-3 ² :5 ¹ /1860	5	19.64	31.42				
6/60:35:T-3 ¹ :5 ² /1860	5	19.64	31.42				
6/60:35:T-3 ³ :5 ² /1860	5	19.64	31.42				
6/60:35:T-3 ² :5 ³ /1860	5	19.64	31.42				
6/60:40:T-3 ³ /1860	3	7.07	18.80	0	26 168	7 531 343	1 275
6/60:40:T-5 ³ /1860	5	19.64	31.42				
6/60:40:T-3 ⁵ /1860	3	7.07	18.80				
6/60:40:T-5 ⁵ /1860	5	19.64	31.42				
6/60:40:T-3 ² :5 ¹ /1860	5	19.64	31.42				
6/60:40:T-3 ¹ :5 ² /1860	5	19.64	31.42				
6/60:40:T-3 ³ :5 ² /1860	5	19.64	31.42				
6/60:40:T-3 ² :5 ³ /1860	5	19.64	31.42				

$d_{b(max)}$: Maximum diameter of the wires used (3mm ó 5mm)

a_p : Area of the wire with the smallest diameter (mm^2)

p : Bonding perimeter of the wire with the smallest diameter(mm)

e_o : Eccentricity of the wires with respect to the centroid of the precast concrete section (mm)

A_{pl} : Gross area of the precast concrete section(mm^2)

I_{pl} : Centroidal moment of inertia of the precast concrete section (mm^4)

p_{pl} : Perimeter of the precast concrete section(mm)

Consideraciones generales:

- Concrete strength at 28 days: ($f'_c = 25MPa$)
- Detensioning: 3 days($\beta_j = 0.6$)
- Weight of the screed: ($q_c = 60 kg/m = 0.6 N/m m$)
- Superimposed dead load (excluding the screed weight):($q_s = 100 kg/m = 1 N/m m$)
- Modulus of elasticity of prestressed steel: ($E_p = 2 \cdot 10^5 MPa$)
- Ambient relative humidity:($HR = 80\%$)
- Abrupt prestress transfer($\alpha_1 = 1.25$)
- Normal-hardening cement:($s = 0.25$)
- Steel stress ratios: ($\xi = f_{py}/f_{pu} = 0.85 \Rightarrow \lambda_t = f_{pj}/f_{pu} = 0.80$)
- The precast slab has no transverse reinforcement: ($\alpha_2 = 1.0$)
- Precast slab reinforcement consists of high-yield strength wires: ($\alpha_3 = 0.7$ y $\eta_1 = 1.4$)
- In all cases, the reinforcement of the precast slab is less than 250 mm from the bottom: ($\eta_2 = 1.0$)
- Low-relaxation steel (for $\lambda_t = 0.80$)

$$f_{pu} = 1770MPa: \begin{cases} K_{re} = 31.9MPa \\ J = 0.037 \\ C = 1.28 \end{cases}$$

$$f_{pu} = 1860MPa: \begin{cases} K_{re} = 34.4MPa \\ J = 0.04 \\ C = 1.28 \end{cases}$$

During the study of losses, the following are modified:

- Precast slab typology:: PPCC: 6/60:30 , PPCC: 6/60:35 y PPCC: 6/60:40
- Reinforcement typology:: T-3³, T-5³, T-3⁵, T-5⁵, T-3²:5¹, T-3¹:5² y T-3²:5³
- Ultimate steel strength: $f_{pu} = 1770MPa$ ó $1860MPa$
- Length of the precast slab (extremes): $l = 3.00m$ y $4.50m$
- Section analyzed: Extreme end of the transfer zone (only for elastic shortening loss) and central section. Table 4 presents the losses at the extreme section during transfer for the HTSC and PPCC models.

Tabla 4. Pérdida en la *sección extrema de transferencia* en prelosas de longitud $l = 3.0m$

TYPOLOGY PPCC		$l = 3.0m$	$HR = 80\%$	$q_{sd} = 1.6 N/m m$	$\lambda_t = 0.80$	$f'_c = 25MPa$					
		$f_{pu} = 1770MPa$					$f_{pu} = 1860MPa$				
		INITIAL	DEFERRED				INITIAL	DEFERRED			
		Δf_{ES} (MPa)	Δf_{CR} (MPa)	Δf_{SH} (MPa)	Δf_{RE} (MPa)	$\Delta f_{diferida}$ (MPa)	Δf_{ES} (MPa)	Δf_{CR} (MPa)	Δf_{SH} (MPa)	Δf_{RE} (MPa)	$\Delta f_{diferida}$ (MPa)
6/60:30	T-3 ³	14,3	25,6	31,5	37,5	94,6	15,0	26,7	31,5	40,3	98,5
	T-5 ³	39,6	64,8	31,5	34,4	130,7	41,7	68,0	31,5	36,8	136,3
	T-3 ⁵	23,8	40,3	31,5	36,3	108,1	25,0	42,2	31,5	39,0	112,7
	T-5 ⁵	66,1	105,7	31,5	31,2	168,4	69,4	110,9	31,5	33,2	175,6
	T-3 ² :5 ¹	22,7	38,7	31,5	36,4	106,6	23,9	40,5	31,5	39,1	111,1
	T-3 ¹ :5 ²	31,2	51,8	31,5	35,4	118,7	32,8	54,2	31,5	38,0	123,7
	T-3 ³ :5 ²	40,7	66,5	31,5	34,3	132,2	42,8	69,7	31,5	36,7	137,8
T-3 ² :5 ³	49,2	79,6	31,5	33,2	144,3	51,7	83,4	31,5	35,5	150,4	

6/60:35	T-3 ³	12,5	19,4	31,4	37,8	88,6	13,2	20,4	31,4	40,7	92,4
	T-5 ³	34,8	53,8	31,4	35,1	120,3	36,6	56,6	31,4	37,7	125,6
	T-3 ⁵	20,9	32,3	31,4	36,8	100,5	22,0	34,0	31,4	39,6	104,9
	T-5 ⁵	58,0	89,7	31,4	32,3	153,4	61,0	94,3	31,4	34,5	160,1
	T-3 ² :5 ¹	20,0	30,9	31,4	36,9	99,2	21,0	32,4	31,4	39,7	103,5
	T-3 ¹ :5 ²	27,4	42,4	31,4	36,0	109,8	28,8	44,5	31,4	38,7	114,5
	T-3 ³ :5 ²	35,7	55,3	31,4	35,0	121,7	37,6	58,1	31,4	37,5	127,0
	T-3 ² :5 ³	43,2	66,8	31,4	34,1	132,3	45,4	70,2	31,4	36,5	138,0
6/60:40	T-3 ³	11,4	17,6	31,2	38,0	86,8	11,9	18,5	31,2	40,9	90,5
	T-5 ³	31,5	48,8	31,2	35,6	115,5	33,1	51,2	31,2	38,1	120,6
	T-3 ⁵	18,9	29,3	31,2	37,1	97,5	19,9	30,8	31,2	39,8	101,8
	T-5 ⁵	52,5	81,3	31,2	33,0	145,5	55,2	85,4	31,2	35,2	151,8
	T-3 ² :5 ¹	18,1	28,0	31,2	37,2	96,3	19,0	29,4	31,2	40,0	100,5
	T-3 ¹ :5 ²	24,8	38,4	31,2	36,4	105,9	26,1	40,3	31,2	39,0	110,6
	T-3 ³ :5 ²	32,4	50,1	31,2	35,5	116,7	34,0	52,6	31,2	38,0	121,8
	T-3 ² :5 ³	39,1	60,5	31,2	34,6	126,3	41,1	63,5	31,2	37,1	131,8

Table 5. Loss in the critical section ($z = L/4$) in precast slabs with a length of $l = 3.0m$

TIPOLOGY PPCC		$l = 3.0m$		$HR = 80\%$			$q_{sd} = 1.6 N/m m$		$\lambda_t = 0.80$		$f'_c = 25MPa$	
		$f_{pu} = 1770MPa$					$f_{pu} = 1860MPa$					
		INITIA L	DEFERRED				INITIA L	DEFERRED				
		Δf_{ES} (MPa)	Δf_{CR} (MPa)	Δf_{SH} (MPa)	Δf_{RE} (MPa)	$\Delta f_{diferida}$ (MPa)	Δf_{ES} (MPa)	Δf_{CR} (MPa)	Δf_{SH} (MPa)	Δf_{RE} (MPa)	$\Delta f_{diferida}$ (MPa)	
6/60:30	T-3 ³	15,0	26,7	31,5	37,4	95,6	15,7	27,9	31,5	40,2	99,5	
	T-5 ³	40,4	66,0	31,5	34,3	131,8	42,4	69,1	31,5	36,7	137,3	
	T-3 ⁵	24,5	41,5	31,5	36,2	109,2	25,7	43,3	31,5	38,9	113,7	
	T-5 ⁵	66,8	106,8	31,5	31,1	169,4	70,1	112,0	31,5	33,1	176,6	
	T-3 ² :5 ¹	23,5	39,8	31,5	36,3	107,7	24,6	41,6	31,5	39,0	112,1	
	T-3 ¹ :5 ²	31,9	52,9	31,5	35,3	119,7	33,5	55,3	31,5	37,9	124,7	
	T-3 ³ :5 ²	41,4	67,6	31,5	34,2	133,3	43,5	70,8	31,5	36,6	138,9	
	T-3 ² :5 ³	49,9	80,7	31,5	33,2	145,3	52,4	84,6	31,5	35,4	151,5	
6/60:35	T-3 ³	12,5	19,4	31,4	37,8	88,6	13,2	20,4	31,4	40,7	92,4	
	T-5 ³	34,8	53,8	31,4	35,1	120,3	36,6	56,6	31,4	37,7	125,6	
	T-3 ⁵	20,9	32,3	31,4	36,8	100,5	22,0	34,0	31,4	39,6	104,9	
	T-5 ⁵	58,0	89,7	31,4	32,3	153,4	61,0	94,3	31,4	34,5	160,1	
	T-3 ² :5 ¹	20,0	30,9	31,4	36,9	99,2	21,0	32,4	31,4	39,7	103,5	
	T-3 ¹ :5 ²	27,4	42,4	31,4	36,0	109,8	28,8	44,5	31,4	38,7	114,5	
	T-3 ³ :5 ²	35,7	55,3	31,4	35,0	121,7	37,6	58,1	31,4	37,5	127,0	
	T-3 ² :5 ³	43,2	66,8	31,4	34,1	132,3	45,4	70,2	31,4	36,5	138,0	
6/60:40	T-3 ³	11,4	17,6	31,2	38,0	86,8	11,9	18,5	31,2	40,9	90,5	
	T-5 ³	31,5	48,8	31,2	35,6	115,5	33,1	51,2	31,2	38,1	120,6	
	T-3 ⁵	18,9	29,3	31,2	37,1	97,5	19,9	30,8	31,2	39,8	101,8	
	T-5 ⁵	52,5	81,3	31,2	33,0	145,5	55,2	85,4	31,2	35,2	151,8	
	T-3 ² :5 ¹	18,1	28,0	31,2	37,2	96,3	19,0	29,4	31,2	40,0	100,5	
	T-3 ¹ :5 ²	24,8	38,4	31,2	36,4	105,9	26,1	40,3	31,2	39,0	110,6	

	T-3 ³ :5 ²	32,4	50,1	31,2	35,5	116,7	34,0	52,6	31,2	38,0	121,8
	T-3 ² :5 ³	39,1	60,5	31,2	34,6	126,3	41,1	63,5	31,2	37,1	131,8

Table 6. Loss in the extreme transfer section in precast slabs of varying lengths $l = 4.50m$

TIPOLOGY PPCC		$l = 4.50m$		$HR = 80\%$		$q_{sd} = 1.6 N/m m$		$\lambda_t = 0.80$		$f'_c = 25MPa$			
		$f_{pu} = 1770MPa$						$f_{pu} = 1860MPa$					
		INITIA L		DEFERRED				INITIA L		DEFERRED			
		Δf_{ES} (MPa)	Δf_{CR} (MPa)	Δf_{SH} (MPa)	Δf_{RE} (MPa)	$\Delta f_{diferida}$ (MPa)	Δf_{ES} (MPa)	Δf_{CR} (MPa)	Δf_{SH} (MPa)	Δf_{RE} (MPa)	$\Delta f_{diferida}$ (MPa)		
6/60:30	T-3 ³	14,3	30,0	31,5	37,2	98,8	15,0	31,2	31,5	40,1	102,7		
	T-5 ³	39,6	69,3	31,5	34,2	134,9	41,7	72,4	31,5	36,6	140,5		
	T-3 ⁵	23,8	44,8	31,5	36,1	112,3	25,0	46,6	31,5	38,8	116,9		
	T-5 ⁵	66,1	110,1	31,5	31,0	172,6	69,4	115,3	31,5	33,0	179,8		
	T-3 ² :5 ¹	22,7	43,1	31,5	36,2	110,8	23,9	44,9	31,5	38,9	115,3		
	T-3 ¹ :5 ²	31,2	56,2	31,5	35,2	122,9	32,8	58,6	31,5	37,7	127,9		
	T-3 ³ :5 ²	40,7	70,9	31,5	34,1	136,5	42,8	74,1	31,5	36,4	142,0		
	T-3 ² :5 ³	49,2	84,0	31,5	33,0	148,5	51,7	87,9	31,5	35,3	154,6		
6/60:35	T-3 ³	12,5	19,4	31,4	37,8	88,6	13,2	20,4	31,4	40,7	92,4		
	T-5 ³	34,8	53,8	31,4	35,1	120,3	36,6	56,6	31,4	37,7	125,6		
	T-3 ⁵	20,9	32,3	31,4	36,8	100,5	22,0	34,0	31,4	39,6	104,9		
	T-5 ⁵	58,0	89,7	31,4	32,3	153,4	61,0	94,3	31,4	34,5	160,1		
	T-3 ² :5 ¹	20,0	30,9	31,4	36,9	99,2	21,0	32,4	31,4	39,7	103,5		
	T-3 ¹ :5 ²	27,4	42,4	31,4	36,0	109,8	28,8	44,5	31,4	38,7	114,5		
	T-3 ³ :5 ²	35,7	55,3	31,4	35,0	121,7	37,6	58,1	31,4	37,5	127,0		
	T-3 ² :5 ³	43,2	66,8	31,4	34,1	132,3	45,4	70,2	31,4	36,5	138,0		
6/60:40	T-3 ³	11,4	17,6	31,2	38,0	86,8	11,9	18,5	31,2	40,9	90,5		
	T-5 ³	31,5	48,8	31,2	35,6	115,5	33,1	51,2	31,2	38,1	120,6		
	T-3 ⁵	18,9	29,3	31,2	37,1	97,5	19,9	30,8	31,2	39,8	101,8		
	T-5 ⁵	52,5	81,3	31,2	33,0	145,5	55,2	85,4	31,2	35,2	151,8		
	T-3 ² :5 ¹	18,1	28,0	31,2	37,2	96,3	19,0	29,4	31,2	40,0	100,5		
	T-3 ¹ :5 ²	24,8	38,4	31,2	36,4	105,9	26,1	40,3	31,2	39,0	110,6		
	T-3 ³ :5 ²	32,4	50,1	31,2	35,5	116,7	34,0	52,6	31,2	38,0	121,8		
	T-3 ² :5 ³	39,1	60,5	31,2	34,6	126,3	41,1	63,5	31,2	37,1	131,8		

The resulting loss values for the Critical Section in PPCC and for HTSC values, in the 4.5 m span length variant, are presented in Table 7.

Table 7. Presents Losses in the Critical Section ($z = l/4$) in Precast Slabs with a Length of $l = 4.50m$

TIPOLOGY PPCC		$l = 4.50m$		$HR = 80\%$		$q_{sd} = 1.6 N/m m$		$\lambda_t = 0.80$		$f'_c = 25MPa$			
		$f_{pu} = 1770MPa$						$f_{pu} = 1860MPa$					
		INITIA L		DEFERRED				INITIA L		DEFERRED			
		Δf_{ES} (MPa)	Δf_{CR} (MPa)	Δf_{SH} (MPa)	Δf_{RE} (MPa)	$\Delta f_{diferida}$ (MPa)	Δf_{ES} (MPa)	Δf_{CR} (MPa)	Δf_{SH} (MPa)	Δf_{RE} (MPa)	$\Delta f_{diferida}$ (MPa)		
6/60:	T-3 ³	15,9	32,6	31,5	37,0	101,1	16,6	33,7	31,5	39,8	105,0		
	T-5 ³	41,3	71,8	31,5	34,0	137,3	43,3	74,9	31,5	36,4	142,8		
	T-3 ⁵	25,4	47,3	31,5	35,9	114,7	26,6	49,2	31,5	38,5	119,2		

	T-5 ⁵	67,7	112,7	31,5	30,8	175,0	71,0	117,9	31,5	32,7	182,1
	T-3 ² :5 ¹	24,4	45,6	31,5	36,0	113,2	25,5	47,4	31,5	38,7	117,6
	T-3 ¹ :5 ²	32,8	58,7	31,5	35,0	125,2	34,4	61,2	31,5	37,5	130,2
	T-3 ³ :5 ²	42,3	73,4	31,5	33,9	138,8	44,4	76,6	31,5	36,2	144,4
	T-3 ² :5 ³	50,8	86,5	31,5	32,8	150,8	53,3	90,4	31,5	35,1	156,9
6/60:35	T-3 ³	12,5	19,4	31,4	37,8	88,6	13,2	20,4	31,4	40,7	92,4
	T-5 ³	34,8	53,8	31,4	35,1	120,3	36,6	56,6	31,4	37,7	125,6
	T-3 ⁵	20,9	32,3	31,4	36,8	100,5	22,0	34,0	31,4	39,6	104,9
	T-5 ⁵	58,0	89,7	31,4	32,3	153,4	61,0	94,3	31,4	34,5	160,1
	T-3 ² :5 ¹	20,0	30,9	31,4	36,9	99,2	21,0	32,4	31,4	39,7	103,5
	T-3 ¹ :5 ²	27,4	42,4	31,4	36,0	109,8	28,8	44,5	31,4	38,7	114,5
	T-3 ³ :5 ²	35,7	55,3	31,4	35,0	121,7	37,6	58,1	31,4	37,5	127,0
	T-3 ² :5 ³	43,2	66,8	31,4	34,1	132,3	45,4	70,2	31,4	36,5	138,0
6/60:40	T-3 ³	11,4	17,6	31,2	38,0	86,8	11,9	18,5	31,2	40,9	90,5
	T-5 ³	31,5	48,8	31,2	35,6	115,5	33,1	51,2	31,2	38,1	120,6
	T-3 ⁵	18,9	29,3	31,2	37,1	97,5	19,9	30,8	31,2	39,8	101,8
	T-5 ⁵	52,5	81,3	31,2	33,0	145,5	55,2	85,4	31,2	35,2	151,8
	T-3 ² :5 ¹	18,1	28,0	31,2	37,2	96,3	19,0	29,4	31,2	40,0	100,5
	T-3 ¹ :5 ²	24,8	38,4	31,2	36,4	105,9	26,1	40,3	31,2	39,0	110,6
	T-3 ³ :5 ²	32,4	50,1	31,2	35,5	116,7	34,0	52,6	31,2	38,0	121,8
	T-3 ² :5 ³	39,1	60,5	31,2	34,6	126,3	41,1	63,5	31,2	37,1	131,8

Smoothed Response Surface for Prestressed Concrete Slab Tension Losses

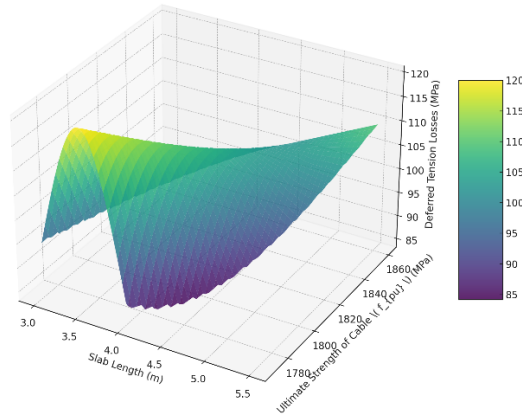


Figure 2 The variations in the increase of tension losses as a function of length.

As the length of the precast slab increases, deferred tension losses increase more significantly. This is reflected in the warmer tones (yellow) observed for lengths greater than 4.5 m.

It is noted that for cables with a higher ultimate strength ($f_{pu} = 1860$ MPa) deferred losses tend to be greater compared to those with ($f_{pu} = 1770$ MPa). This effect is more noticeable in precast slabs with greater lengths, where the internal tension of the cable is more affected by factors such as creep and relaxation.

- The smoothed surface shows a general inclination towards longer lengths and higher f_{pu} values, indicating that these combinations should be given greater consideration in the design of prestressed precast slabs to avoid excessive losses that could compromise the load-bearing capacity and durability of the structural element.

4. Discussion of Results

Fig. 3 provides curves showing tension losses in HTSC for the PPCC models, which facilitates connecting criteria regarding the results of this study

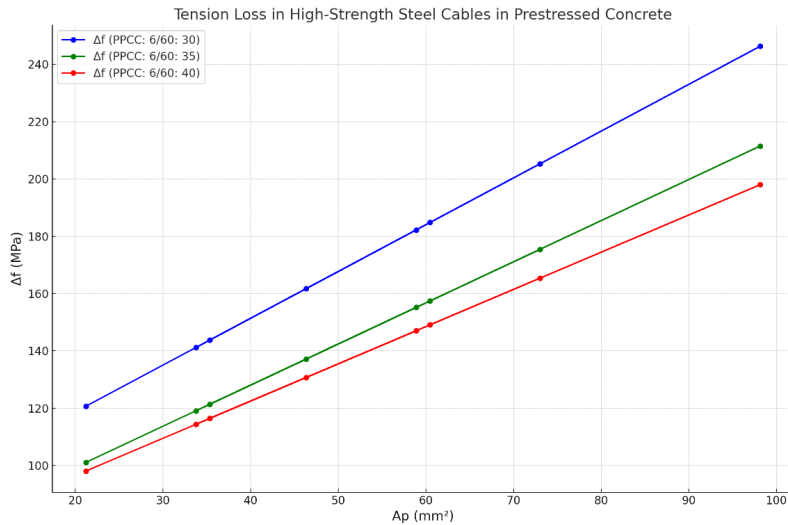


Figure 3. Presents the loss curves for each PPCC model, useful for discussion

The configuration **PPCC: 6/60: 30** has the highest tension losses for any value of A_{pl} , which could indicate that this configuration has higher efficiency in stress transfer or greater intrinsic losses..

The configurations **PPCC: 6/60: 35** and **PPCC: 6/60: 40** show lower tension losses, with the **PPCC: 6/60: 40** configuration being the most efficient among the three. This suggests that this configuration may be preferable in terms of minimizing tension losses..

The positive linear relationship between A_{pl} y Δ_p suggests that as the cross-sectional area of the cable increases, the tension losses also increase. This may be due to the larger amount of material in cables with a greater cross-sectional area, resulting in higher losses due to friction and other factors.

Evaluating tension losses in prestressed concrete HTSC is essential to ensure durability and performance during the operational period. According to [12] tension loss in HTSC induces excessive deflections and cracking of the concrete, compromising the health of the structure and resulting in a reduction of the expected service life of the construction. In this regard, [13] similarly argue that evaluating tension losses is crucial not only for maintaining the load-bearing capacity of the structure but also for anticipating and planning necessary maintenance, thereby ensuring the continuous safety and functionality of the structure.

The **PPCC: 6/60: 30** configuration has the highest tension losses for any value of A_{pl} , which could indicate that this configuration has higher efficiency in stress transfer or greater intrinsic losses. The **PPCC: 6/60: 35** and **PPCC: 6/60: 40** configurations show lower tension losses, with the **PPCC: 6/60: 40** configuration being the most efficient among the three, suggesting that this configuration may be preferable in terms of minimizing tension losses. These design results allow for selecting the appropriate cables (HTSC) for the prestressed concrete element. The relevance of evaluating tension losses in

cables ensures the expected service life during the operational period; otherwise, there is a risk of reducing the lifespan of the entire structure.

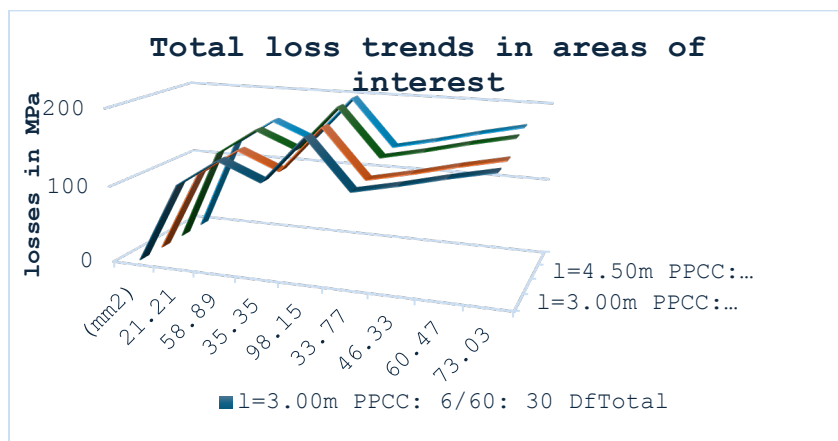


Fig 4. Presents total loss curves in critical and debatable areas.

Proper evaluation of tension losses is crucial for controlling the load-bearing capacity of the structure and anticipating routine maintenance, ensuring the continuous functionality of the structure [13]. In contrast, the PPCC: 6/60: 35 and PPCC: 6/60: 40 models show lower tension losses, with the PPCC: 6/60: 40 model being the most efficient among the three models. According to [14] a proven configuration for tension losses is preferable in terms of minimizing tension losses. Finally, the results provide validity and feasibility to the research.

5. Conclusion

Initially, it is only necessary to distinguish between the transfer section and the critical section, which is tentatively located at a distance of $l/4$ from the support, in the case of the precast slab typology PPCC: 6/60:30. This is the only configuration where, due to the eccentricity of the wires, a convex deformation may occur when the prestressing is transferred. In the other two typologies, the eccentricity of the wires is zero, and the losses that occur in both sections are exactly the same, since in these cases $M_{gz} = 0$.

The results presented in Tables 4 and 5 (for a length of 3.00 m), as well as those in Tables 6 and 7 (for a length of 4.50 m), certify that the influence of bending characterized by the moment $M_{gz} = 0$ is so small that, for practical purposes, the losses that occur in both sections can be considered to be approximately equal. This conclusion allows a single value to be used to estimate the initial and deferred losses that occur.

It is concluded that the greatest losses, both initial and deferred, occur in the weak section of the precast slab reinforced with the highest prestressing load, as shown in Figure 1. The most significant tension losses in prestressing are caused by plastic flow, even delayed, in the concrete. In contrast, the lowest losses are observed in slabs with low amounts of prestressing and elastic shortening of the concrete due to prestressing. It was found that concrete shrinkage and steel relaxation losses are small, especially when they are deferred.

When comparing the ultimate steel tension with the tension losses in the prestressed precast slab, the latter are very low, particularly the initial losses that occur during detensioning. The variables present in the model include: detensioning at 72 hours, relaxation of high-yield strength steel, and a relative humidity of 80%, among others.

It was found that the smoothed surface shows a general inclination towards longer lengths and higher f_{pu} values, indicating that these combinations should be given greater attention in the design of prestressed precast slabs to avoid excessive losses that could compromise the load-bearing capacity and durability of the structural element.

Finally, it is concluded that the presented model is valid for the practical undertaking of manufacturing prestressed precast slabs with a composite screed (PPCC).

References

- [1] Kim, S., Park, J., & Lee, K. (2021). Friction losses in post-tensioned concrete structures. *Structural Concrete*, 22(2), 652-662. <https://doi.org/10.1002/suco.202000243>
- [2] Lee, S., & Lee, J. (2020). Effect of friction on prestressed concrete tendons. *Journal of Materials in Civil Engineering*, 32(6), 04020146. [https://doi.org/10.1061/\(ASCE\)MT.1943-5533.0003175](https://doi.org/10.1061/(ASCE)MT.1943-5533.0003175)
- [3] Park, J., & Lee, S. (2022). Elastic shortening in pretensioned concrete elements. *ACI Structural Journal*, 119(2), 165-174. <https://doi.org/10.14359/51732015>
- [4] Hsiao, J.-K. K., & Hsiao, J.-K. K. ". (2017). Prestress Loss Distributions along Simply Supported Pretensioned Concrete Beams. *Electronic Journal of Structural Engineering*, 16, 18–25. http://opensiuc.lib.siu.edu/cee_pubs
- [5] Zeren, M., & Zeren, M. (2003). Stress relaxation properties of prestressed steel wires. *Journal of Materials Processing Technology*, 141, 86–92. [https://doi.org/10.1016/S0924-0136\(03\)00131-6](https://doi.org/10.1016/S0924-0136(03)00131-6)
- [6] Choi, J., Woods, C., Hrynyk, T., & Bayrak, O. (2018). *MEASURING FRICTION LOSSES OF LARGE-ANGLE POST-TENSIONED CONCRETE WALLS*.
- [7] Hwang, J., Lee, S., & Kim, D. (2022). Relaxation properties of high-strength prestressing steel. *Materials Science and Engineering A*, 827, 141889. <https://doi.org/10.1016/j.msea.2021.141889>
- [8] Lee, J., & Kwon, H. (2021). Long-term relaxation of prestressed steel. *Journal of Constructional Steel Research*, 181, 106624. <https://doi.org/10.1016/j.jcsr.2021.106624>
- [9] Eldin, M. N., Dereje, A. J., & Kim, J. (2020). Seismic Retrofit of Framed Buildings Using Self-Centering PC Frames. *Journal of Structural Engineering*, 146(10). [https://doi.org/10.1061/\(ASCE\)ST.1943-541X.0002786](https://doi.org/10.1061/(ASCE)ST.1943-541X.0002786)
- [10] Pathak, P., & Zhang, Y. X. (2019). Numerical study of structural behavior of fiber-reinforced polymer-strengthened reinforced concrete beams with bond-slip effect under cyclic loading. *Structural Concrete*, 20(1), 97–107. <https://doi.org/10.1002/suco.201800035>
- [11] Cong, P., & Mei, L. (2021). Using silica fume for improvement of fly ash/slag based geopolymer activated with calcium carbide residue and gypsum. *Construction and Building Materials*, 275, 122171. <https://doi.org/10.1016/j.conbuildmat.2020.122171>
- [12] Bonopera, M., Chang, K.-C., & Lee, Z.-K. (2020). State-of-the-Art Review on Determining Prestress Losses in Prestressed Concrete Girders. *Applied Sciences*, 10(20), 7257. <https://doi.org/10.3390/app10207257>
- [13] Moravčík, M., & Kral'ovanec, J. (2022). Determination of Prestress Losses in Existing Pre-Tensioned Structures Using Bayesian Approach. *Materials*, 15(10), 3548. <https://doi.org/10.3390/ma15103548>
- [14] Hamed, E., & Frostig, Y. (2006). Nonlinear dynamic behavior of prestressed beams with unbonded tendons. *Journal of Structural Engineering*, 132(10), 1604-1612. [https://doi.org/10.1061/\(ASCE\)0733-9445\(2006\)132:10\(1604\)](https://doi.org/10.1061/(ASCE)0733-9445(2006)132:10(1604))